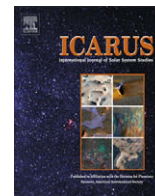




Contents lists available at ScienceDirect

Icarus

journal homepage: www.elsevier.com/locate/icarus

Chemical reactions in the Titan's troposphere during lightning

Tamás Kovács^{a,*}, Tamás Turányi^b

^aSchool of Physics and Astronomy, University of Leeds, Leeds, LS2 9JT West Yorkshire, UK

^bInstitute of Chemistry, Eötvös University (ELTE), Pázmány P. sétány 1/A, H-1117 Budapest, Hungary

ARTICLE INFO

Article history:

Received 14 September 2009

Revised 7 January 2010

Accepted 8 January 2010

Available online xxx

Keywords:

Titan
Lightning

ABSTRACT

In the lower troposphere of the Titan the temperature is about 90 K, therefore the chemical production of compounds in the CH₄/N₂ atmosphere is extremely slow. However, atmospheric electricity could provide conditions at which chemical reactions are fast. This paper is based on the assumption that there are lightning discharges in the Titan's lower atmosphere. The temporal temperature profile of a gas parcel after lightning was calculated at the conditions of 10 km above the Titan's surface. Using this temperature profile, composition of the after-lightning atmosphere was simulated using a detailed chemical kinetic mechanism consisting of 1829 reactions of 185 species. The main reaction paths leading to the products were investigated. The main products of lightning discharges in the Titan's atmosphere are H₂, HCN, C₂N₂, C₂H₂, C₂H₄, C₂H₆, NH₃ and H₂CN. The annual production of these compounds was estimated in the Titan's atmosphere.

© 2010 Elsevier Inc. All rights reserved.

1. Introduction

Saturn's largest moon, Titan became a scientifically interesting object when it turned out that, similarly to the Earth, it has a nitrogen based atmosphere. One of the most significant components of its atmosphere, methane can condense easily at low altitudes, where the temperature is around 90 K and this makes cloud formation possible (Lorenz, 1995). Although so far there is no experimental evidence for lightning at Titan (Fischer et al., 2007), its presence has not been ruled out experimentally and has been predicted theoretically (Tokano et al., 2001). Lightning can generate extremely high temperature and this allows reactions that otherwise can happen only in the higher atmosphere induced by the electrons coming from the Saturn's magnetosphere (McEwan et al., 1998; Bird et al., 1997; Romanzin et al., 2008) or by VUV photons coming from the Sun (Romanzin et al., 2008). According to the hypothesis of Borucki et al. (1984) the lightning energy dissipation rate at the Titan is much lower than at the Earth and from this they concluded that lightning could have more impact on HCN and C₂N₂ formation than solar UV radiation. The plasma, formed by lightning, extinguishes shortly after the lightning and the temperature falls. As a result, more complicated molecules are produced from the methane–nitrogen mixture. Due to the low temperature, the rate of decomposition of these products is negligible and therefore there is a continuous accumulation of these compounds.

Titan was closely investigated by Voyager-1 already in November 1980. However, in the Voyager missions only its main features and the upper atmosphere were studied. The exact chemical composition of the lower atmosphere was not investigated until the Huygens mission in 2005. The Huygens probe revealed (Fulchignoni et al., 2005) the pressure and temperature profiles over the altitude range of 0–1400 km and investigated the atmospheric electricity. The surface pressure determined by the Huygens probe was 1.467 atm and the measured surface temperature was 93.65 K. McKay et al. (1997) estimated the vertical profile of lapse rate from the Voyager ingress and egress radio occultation data and the dry lapse rate was determined to be $dT/dz = -1.3$ K/km. The temperature profile measured by the Huygens–Cassini mission was in agreement with the previously determined temperature gradient in the Titan's troposphere. The troposphere is situated between 0 km and 44 km on the Titan (Fulchignoni et al., 2005).

Tokano et al. (2001) studied the possibility of cloud formation on the Titan by a numerical 1D time-dependent thundercloud model. They found that methane clouds are formed under 20 km, although these are less common than the Earth's water clouds. They stated that the conditions are present for lower tropospheric lightning. Tokano et al. (2006) later showed that there might be methane–nitrogen clouds containing liquid droplets between 8 and 16 km.

Several papers discussed the results of experimental studies of a Titan-like atmosphere in terrestrial laboratories. Fujii and Arai (1999) simulated the conditions of the Titan's upper troposphere with 10 n% methane–90 n% nitrogen mixture in microwave plasma. Microwave plasma was used to emulate the role of the lightning. Besides the predictable HCN, more than two-carbon-atom-containing

* Corresponding author.

E-mail addresses: takovacs@gmail.com (T. Kovács), turanyi@chem.elte.hu (T. Turányi).

amines and nitriles were also found. The product mixture contained more than 70 minor products. Coll et al. (1999) used spark discharge, 0.9 atm pressure, 100 K initial temperature and 11 n% CH₄–89 n% N₂ mixture. They found that in the product mix the C:N ratio is 11:1, while the C:H ratio is around 1:1. The major products were acetylene, hydrogen-cyanide and ethane, with the following average mole fractions: $\chi(\text{C}_2\text{H}_2) = 2.5 \times 10^{-7}$, $\chi(\text{HCN}) = 8.9 \times 10^{-8}$, $\chi(\text{C}_2\text{H}_6) = 1.1 \times 10^{-8}$. The mole fractions of the C₆< compounds were below 10⁻¹⁰, except for the benzene: $\chi(\text{C}_6\text{H}_6) = 1.9 \times 10^{-10}$. In total, 35 C₄< compounds were identified, among which 11 were nitrogen-containing. Borucki et al. (1988) simulated the Titan's lower atmosphere by 1 atm, 3 n% CH₄–97 n% N₂ mixture. The role of lightning was replaced by using laser induced plasma. At these conditions the following main products were formed: HCN, C₂H₂, C₂H₄, C₂H₆ and C₃H₈.

In the last decade several theoretical studies have been carried out on the Titan's atmosphere. These included the investigation of the condensation processes in the Titan's stratosphere (de Kok et al., 2008), the dynamical behavior of the stratosphere (Crespin et al., 2008) and simulating the Titan's atmosphere by discharge experiments (Pereira et al., 2008; Plankensteiner et al., 2007). In our case the most relevant is the study of Borucki et al. (1984), in which the authors used thermodynamic equilibrium calculations to predict the product distribution of the reactions induced by lightning discharges and they predicted that, besides HCN and C₂N₂, large amount of solid carbon is also formed in the reaction.

The motivation of the present study is to determine a more accurate product yield distribution of the reactions initiated by lightning using a chemical kinetic model. As it will be discussed later, thermodynamic models cannot give correct results at low temperatures, and therefore carrying out chemical kinetic simulations is essential.

2. Product distribution from chemical reactions after lightning

No detailed information is available on the lightning discharges of the Titan, therefore in the simulations similar characteristics to the Earth's lightning discharges were assumed.

The temporal temperature profile after lightning was calculated in the following way. We assumed that lightning produced a high temperature gas cylinder, having diameter of 0.025 m and initial temperature of 30,000 K. This is an estimated maximum temperature within a lightning channel (McGraw Hill, 1997). The assumed initial composition of the gas was 95% N₂ and 5% CH₄. From the Huygens mission it was concluded (Niemann et al., 2005) that at 8 km altitude the troposphere contains approximately 4.9% methane.

The heat conductivity equation related to cylindrical symmetry (Landau and Lifshitz, 1987) was used to calculate the temporal and spatial temperature profiles. The temperature profile was obtained numerically via solving the partial differential equation related to the cooling.

$$\frac{\partial T}{\partial t} = \frac{\lambda(T)}{C_p(T)\rho(T)} \left(\frac{\partial^2 T}{\partial r^2} + \frac{1}{r} \frac{\partial T}{\partial r} \right) + \frac{1}{C_p\rho(T)} \text{grad } \lambda(T) \text{grad } T \quad (1)$$

where T is temperature, r is the spatial co-ordinate, t is time and $C_p(T)$, $\rho(T)$, and $\lambda(T)$ are the temperature dependent functions of heat capacity, density, and heat conductivity, respectively. This equation was solved numerically using a custom made computer code (Lagzi, personal communication, 2008; Izsák and Lagzi, 2005). Note that value given by the second term of the right hand side is about five orders of magnitude smaller than by the first term, therefore this term was neglected in the simulations and the following simplified equation was used:

$$\frac{\partial T}{\partial t} = \frac{\lambda(T)}{C_p(T)\rho(T)} \left(\frac{\partial^2 T}{\partial r^2} + \frac{1}{r} \frac{\partial T}{\partial r} \right) \quad (2)$$

The temperature of the surrounding gas at infinite distance was set to 81 K, which corresponds to the temperature at 10 km altitude in the troposphere. Solving this equation requires knowing the temperature dependence of the heat capacity C_p , density ρ , and heat conductivity λ . Since the atmosphere contains mainly (95 n%) nitrogen, the N₂ data for C_p , ρ , λ were used. The corresponding temperature dependent data were collected from the literature (CRC Handbook of Chemistry and Physics, 1994–1995; Friend et al., 1987; Stephen et al., 1989). The calculations were carried out at $r = 1$ cm relative to the center of the lightning channel.

The lightning generates an intense sound wave. Then, the plasma formed from the surrounding gas rapidly expands and a shock wave is generated. For this, at the moment of the lightning the pressure can reach even 30 atm. However, in a few microseconds this falls back to the initial pressure (Finke, 2007). Therefore, the timescale of the pressure fall is much shorter than of the temperature fall to the ambient temperature. For this reason, in our simulations steady-state pressure was assumed and the pressure used was constant 0.92 atm that corresponds to 10 km distance from the surface. At this elevation, cloud formation, which is essential for lightning discharges, may happen (Tokano et al., 2001, 2006).

The maximum temperature of the lightning is uncertain, but it does not cause an uncertainty in the chemical calculations. As the temperature of the gas parcel decreases, the composition of the gas can be determined by thermodynamic equilibrium calculations. Above a threshold temperature, the results of kinetic and thermodynamic calculations are in accordance. This threshold temperature is in the range of 2500–3000 K, depending on the chemical system. Below this threshold temperature, the correct composition can be calculated by chemical kinetic simulations only (Kovács et al., 2005, 2006). To be on the safe side, in our calculations the concentration changes were simulated from the time when the temperature of the gas had fallen below 5100 K. The calculated temperature profile is shown in Fig. 1, and the numerical results are given in Table 1.

The chemical kinetic simulations were carried out using a detailed reaction mechanism that was assembled in the following way. We utilized the detailed reaction mechanism of Dean and co-workers (Sheng and Dean, 2004; Gupta et al., 2006) that is able to describe partial oxidation and pyrolysis of methane up to high conversion. This mechanism is available from our Web site (SEM, 2009). The original mechanism contains 3418 reversible and 38

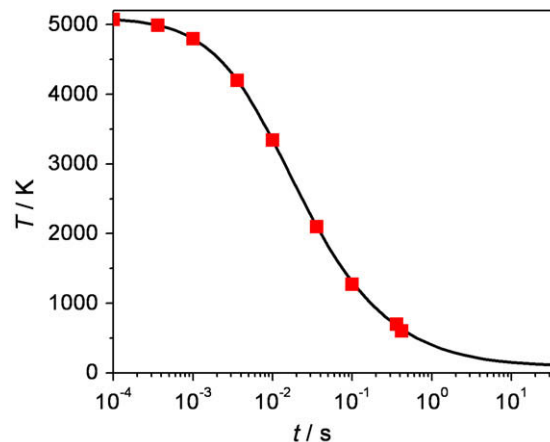


Fig. 1. Post-lightning temperature profile.

Table 1Numerical values of the post-lightning temperature profile calculated for N₂.

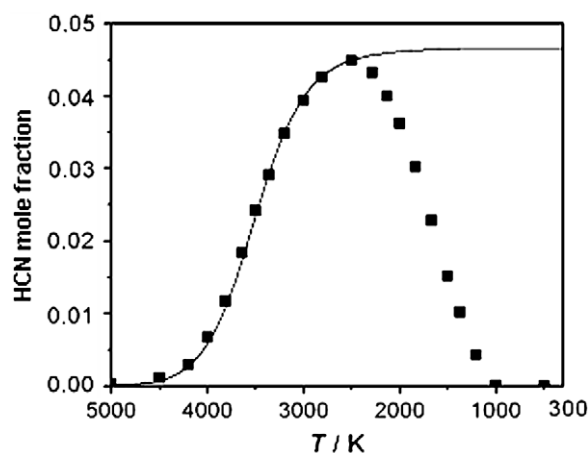
Time (s)	Temperature (K)
0.00	5100
1.00 × 10⁻⁴	5075
3.60 × 10⁻⁴	4989
1.00 × 10⁻³	4799
3.60 × 10⁻³	4198
6.10 × 10 ⁻³	3792
1.00 × 10⁻²	3342
3.60 × 10⁻²	2100
0.100	1275
0.360	700
0.416	605
0.648	500
1.000	400
1.790	300
4.530	200
50.00	100

irreversible reactions of 348 C-, H- and O-containing reactive species. This mechanism was converted to an irreversible-only mechanism by using MECHMOD (MECHMOD, 2003) and thus a mechanism containing 6914 irreversible reactions was obtained. In the next step, all the O-containing species and their reactions were removed by MECHMOD and in this way a mechanism containing 1618 irreversible reactions and 168 reactive species was obtained. Then, reactions of N-containing species (N₂, CN, H₂CN, N, NH, HCN, NH₂, C₂N₂, NNH, NH₃, N₂H₂, N₂H₃, N₂H₄, CNN, HCNN, HCNH, NCN) were added to the model, based on the updated high-temperature nitrogen chemistry mechanism used by Zsély et al. (2008). The final mechanism contains 1829 irreversible reactions of 185 reactive species. Ionic and electron impact reactions were not included in the mechanism. These reactions play an important role only in the thermosphere of the Titan, where the highly energetic electrons originating from the Saturn's magnetosphere initiate ionization. In the lightning, ion-containing plasma is formed, but below 5000 K the ion concentration is small and therefore the rates of the ionic reactions are negligible.

To take into account non-equilibrium chemistry, the simulations were carried out in the following way. First, the thermodynamic equilibrium composition was determined by program EQUIL (EQUIL, 2009) at 5100 K. Then, chemical kinetic calculations with the time dependent temperature profile of Fig. 1 were performed using program SENKIN (SENKIN, 1988) at constant pressure of 0.92 atm.

The model does not include material transport processes, since the transport effects have significantly slower timescale, and therefore do not play an important role. They would have effect in the expanding shock where material transport is fast enough, however in the low temperature region usually only thermal diffusion takes place.

The final time of simulations was 50 s, which corresponds to 100 K final temperature. The concentrations of the stable species did not change after this time. Results for HCN mole fractions are shown in Fig. 2. The squares indicate the thermodynamic equilibrium composition, belonging to the given temperature. The solid line indicates the concentration profile obtained from chemical kinetic simulations in a gas parcel that is cooled down according to the temperature profile given in Fig. 1. Above about 2500 K, the two calculations gave identical concentrations, but below this threshold temperature the calculated concentrations are very different. Table 2 shows that the main products of lightning are HCN, C₂N₂ and H₂. Note, that CH₄ was completely destroyed, but some of it (<0.1%) reformed at low temperatures. Mole fractions and yields corresponding to 700 K are summarized in Table 2.

**Fig. 2.** Comparison of the thermodynamic (squares) and kinetic (solid line) calculations for the concentration of HCN.**Table 2**

Mole fractions, yields and annual yields obtained in the simulations.

	Mole fraction	Yield (%)	Annual yield (mol)
H ₂	4.8×10^{-2}	96	4.10×10^3
HCN	4.7×10^{-2}	94	4.02×10^3
C ₂ N ₂	2.7×10^{-6}	<0.1	2.31×10^{-1}
C ₂ H ₂	2.6×10^{-6}	<0.1	2.23×10^{-1}
C ₂ H ₄	1.9×10^{-6}		1.62×10^{-1}
C ₂ H ₆	4.1×10^{-7}		3.51×10^{-2}
NH ₃	1.2×10^{-8}		1.03×10^{-3}
H ₂ CN	1.1×10^{-6}		9.47×10^{-2}

In the section below we try to estimate the annual production of the various compounds in the Titan's atmosphere due to lightning. There is little uncertainty in the initial gas composition and the chemistry, but there is significant uncertainty in the number and characteristics of the Titan's lightning discharges. However, the data below may provide a first estimation.

No data were found about the properties of the lightning in the Titan. Therefore, we assumed similar characteristics to the lightning on the Earth. According to Christian (1999), there are 1.65 billion cloud-to-cloud and 165 million cloud-to-ground lightning discharges per year in the Earth. Only cloud-to-ground lightning discharges were considered. In (Fischer et al., 2007) the estimated upper limit for the lightning frequency on the Titan is 10^{-6} flashes per second, which results in 32 lightning discharges per year on the Titan. The lightning channel diameter was assumed to be 5 cm (McGraw-Hill, 1997) and its length 10 km. Therefore, the volume of a lightning channel is 19.63 m^3 . The temperature at the surface of the Titan is about 94 K, while at 10 km elevation about 81 K, the average temperature along the channel was assumed to be 85 K. The molar volume at 85 K and 0.92 atm pressure is $7.342 \times 10^{-3} \text{ m}^3$. This means that initially 2674 mol compounds (133.7 mol methane and 2540.3 mol nitrogen) are present in the lightning channel.

The annual yield n was calculated by the following expression:

$$n = \frac{xNlr^2\pi}{V_m} \quad (3)$$

where V_m is the molar volume, x is the mole fraction of the actual product given in Table 2, N is the number of lightning per annum, l is the length of the lightning channel and r is the radius of the lightning channel. The results are given in Table 2. We repeat, this is a crude estimation, where the greatest uncertainty is in the annual number and average length of the lightning discharges. Using

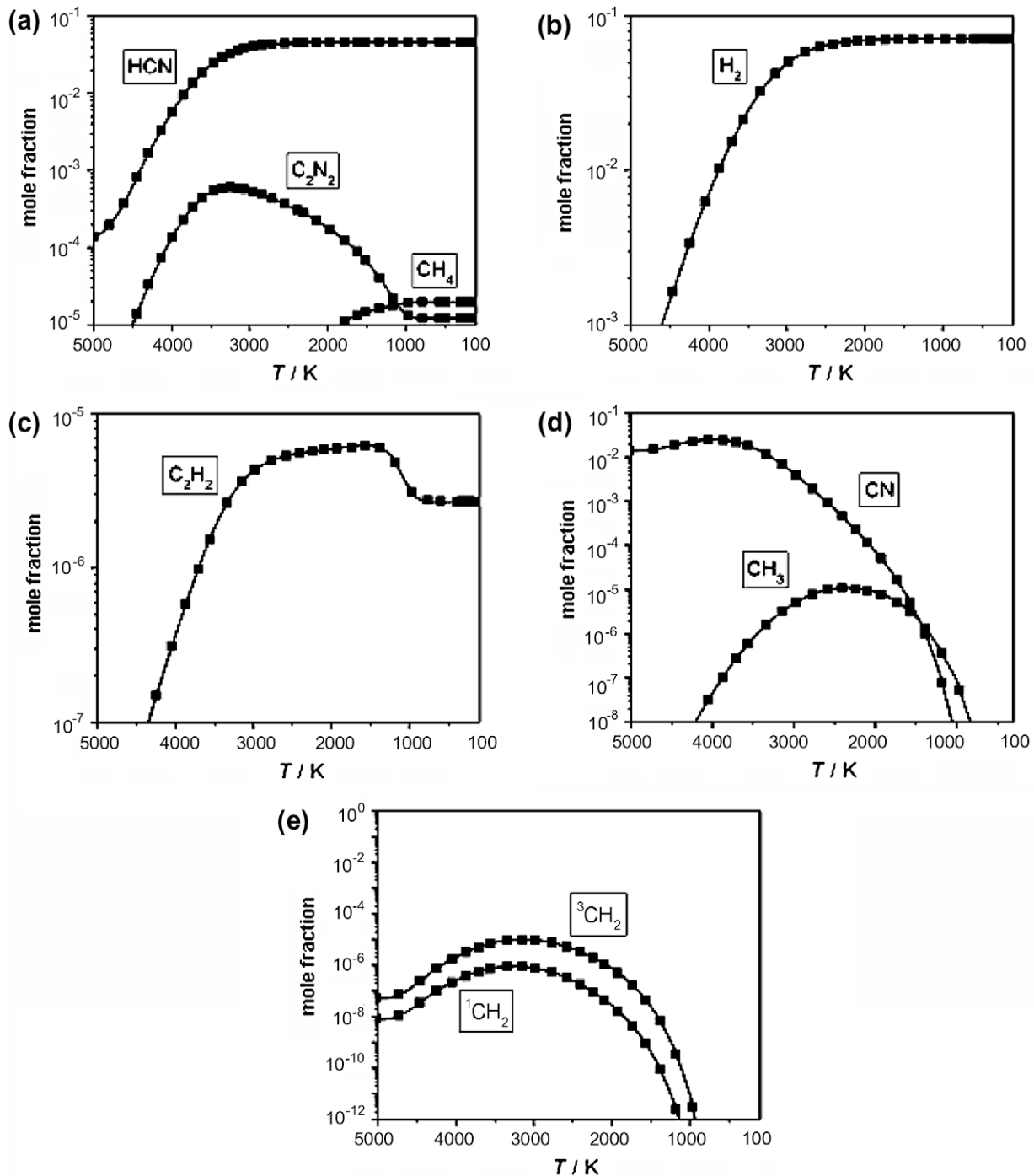


Fig. 3. Concentration profiles obtained by the full (solid lines) and the reduced (squares) mechanisms.

Eq. (2), the annual production of the various compounds can be recalculated when more information will be available on the number and characteristics of lightning discharges on the Titan.

Our results are very different from those of Borucki et al. (1984). Although Borucki et al. did not provide detailed quantitative information on the product yield, they found that solid carbon formation is significant. From their thermodynamic model they concluded that the mole fraction of solid carbon is about 10^{-3} at 500 K, while that of the HCN is negligible. Note, that the authors carried out the simulations in the temperature range of 500–5000 K, although the temperature in the Titan's troposphere is much lower, around 90 K. Also, it is important to note

that our previous studies (Kovács et al., 2005; Kovács and Deam, 2006) indicated that at lower temperatures the thermodynamic simulations give false results since below 3000 K the chemical reactions are slow and there is no time to reach the thermodynamic equilibrium. This opinion is also supported by the comparison of the results of thermodynamic equilibrium calculations of Borucki et al. (1984) and the outcomes of the parallel experimental studies of Borucki et al. (1988). They predicted significant solid carbon formation and no HCN formation in the thermodynamic calculations, while the experimental results indicated no solid carbon but the formation of significant amount of acetylene and hydrogen-cyanide.

The results of our calculations can be compared with the experimental ones by Borucki et al. (1988). Borucki et al. used laser induced plasma to simulate lightning discharges. However, their experiments were carried out at 298 K, which is much higher than the temperature of the Titan's troposphere. The results of Borucki et al. are partially in agreement with ours since they also found significant production of HCN and lack of solid carbon. A significant difference is that Borucki et al. observed approximately identical HCN and C_2H_2 yields. They did not measure the production of C_2N_2 .

3. Kinetic analysis chemical reactions after lightning

Kinetic analysis was carried out in seven time points, which were chosen to be equidistant over the range of 10^{-4} s and 0.1 s in a logarithmic scale. The chosen times are given by bold figures in Table 1 and they are indicated with squares in Fig. 1. The main products that are species H_2 , CH_4 , HCN, C_2N_2 , C_2H_2 , C_2H_4 and H_2CN were considered important. The mechanism reduction was carried out by program KINALC (KINALC, 2005), using options CONNECT and PCAF. The reduced mechanism contained only 146 irreversible reactions of 40 species. The obtained reduced mechanism is available in Appendix A. It is important to note that the methylene and NCN-reactions are turned out to be important. Fig. 3a–e shows the concentration change of the most important radicals having mole fractions higher than 10^{-8} and of the products having mole fractions higher than 10^{-5} . Solid lines show the results obtained with the full mechanism, while squares with the reduced mechanism. The concentrations obtained by the reduced mechanism are always within 1% identical with the ones obtained by the full model.

Fluxes of C and N atoms were investigated in the seven selected points. Flux of an atom is defined as the sum of the rates of all reaction steps that convert the given species to another, multiplied by the change of the number of atoms investigated (Revel et al., 1994). The net flux is the difference of the two reverse fluxes and these net fluxes are plotted and discussed below. It is interesting that the dominant flux of the methane decomposition is the $CH_4 \rightarrow HCN$ process. Fig. 4 shows the C-atom fluxes at 2310 K, where the concentration of methylene, which is one of the most important radicals, is the highest. The flux figures were created using code FluxViewer (FluxViewer, 2007).

Radicals CH_3 , CN, 1CH_2 and 3CH_2 have significant fluxes till 750 K, which indicates the importance of these radicals. This is in accordance with the concentration profiles, which do not change below 700 K. The dominant flux of the methyl generation is the $^3CH_2 \rightarrow CH_3$ conversion, while the main consumption flux goes via the 1CH_2 form. Above 2650 K the singlet methylene also takes part in the H_2CN formation. The fluxes of the CN radical are still rel-

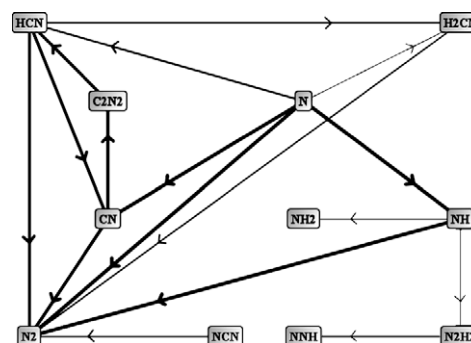


Fig. 5. N-atom fluxes for methane–nitrogen system calculated at 2310 K.

atively significant at 1000 K; at this point only the CH, the C_2N_2 and HCN have major fluxes. The reactions of singlet methylene have significant fluxes even below 1200 K, since the spin forbidden $^1CH_2 + N_2 \rightarrow ^3CH_2 + N_2$ collision induced intersystem crossing has relevant fluxes at these conditions.

In order to clarify the role of the ammonia and its derivatives, N-atom fluxes were also analyzed. Fig. 5 shows the N-atom fluxes at 2310 K. Below this temperature the reactions of the ammonia do not have importance.

At high temperature, much N and CN are formed via reactions $NNH \rightarrow N + NH$ and $HCN \rightarrow H + CN$. In the temperature range 3500–2400 K, CN and N are converted to HCN and C_2N_2 , while at lower temperature the CN radical is consumed mainly in reactions in which nitrogen molecule is formed during which reactions of C_2N_2 and HCN molecules have major role. The flux of the $NCN \rightarrow N_2$ process is significant even at 1560 K, but below this its importance, together with the $HCN \rightarrow H_2CN$ and $N_2 \rightarrow H_2CN$ processes, decreases.

4. Conclusions

Articles related to the chemical processes present in the lower atmosphere of the Titan were reviewed. On the basis of these articles, simulations were planned to model the reactions taking place in the lower atmosphere of the Titan initiated by possible lightning. Relatively precise information is available for the atmospheric composition and conditions. According to the results of reaction kinetic simulations, HCN is definitely the most important product of lightning. Annual productions of the various compounds due to lightning on the Titan were estimated. During the simulations carried out for the Titan conditions (CH_4 – N_2 system), not only product distribution was calculated, but a detailed reaction kinetic analysis was also carried out. The original detailed reaction mechanism containing 1829 irreversible reactions of 185 reactive species could be reduced to a mechanism containing 146 irreversible reactions of 40 species, while the simulated concentrations of the important species remained identical within 1%. Investigation of the C and N-atom fluxes indicated that only the one- and two-carbon-atom-containing hydrocarbon derivatives, the CN radical and the two forms of the methylene (1CH_2 and 3CH_2) have significant role.

Acknowledgments

The authors thank the support of OTKA T68256, the suggestions of Dr. I. Gy. Zsély on the NO_x chemistry, and the help of Dr. I. Lagzi in the numerical solution of the thermal conductivity equation.

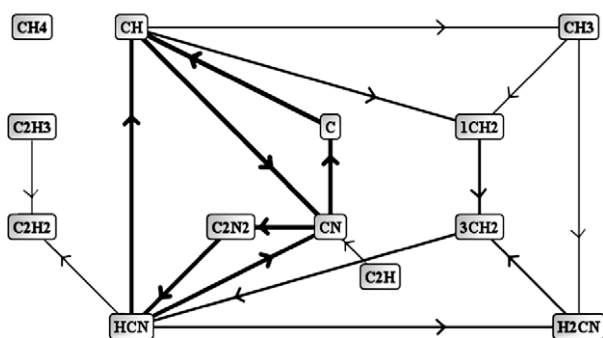


Fig. 4. C-atom fluxes at temperature 2310 K.

Appendix A

Reduced mechanism

CH ₄ -N ₂ Reduced mechanism	$(k = A T^{**} b \exp(-E/RT))$		
	A	b	E
1. H + C ₂ H ₃ ⇒ C ₂ H ₂ + H ₂	1.21E+13	.0	.0
2. C ₂ H ₂ + H ₂ ⇒ H + C ₂ H ₃	2.82E+11	.7	67964.2
3. CH ₃ +C ₂ H ₅ ⇒ CH ₄ + C ₂ H ₄	1.15E+12	.0	.0
4. 2C ₂ H ₅ ⇒ C ₂ H ₄ + C ₂ H ₆	6.00E+13	-.6	.0
5. C ₂ H ₅ + CBCCF ⇒ C ₂ H ₄ + CBCC	3.00E+12	.0	.0
6. C ₂ H ₅ + CWCCF ⇒ C ₂ H ₄ + CWCC	3.00E+12	.0	.0
7. 2CH ₃ ⇒ C ₂ H ₆	9.12E+40	-8.6	10419.6
8. C ₂ H ₆ ⇒ 2CH ₃	3.02E+52	-10.9	104364.2
9. 2CH ₃ ⇒ C ₂ H ₅ + H	1.32E+17	-1.3	16106.2
10. C ₂ H ₅ + H ⇒ 2CH ₃	4.08E+22	-2.6	6130.3
11. CBCC + H ⇒ CH ₃ + C ₂ H ₄	2.41E+31	-5.2	16233.5
Declared duplicate reaction...			
12. CBCC + H ⇒ CH ₃ + C ₂ H ₄	4.67E+44	-9.0	25866.7
Declared duplicate reaction...			
13. CWCCCF ⇒ C ₂ H + C ₂ H ₄	3.84E+56	-13.3	51188.7
14. C ₂ H + C ₂ H ₄ ⇒ CWCCCF	2.35E+47	-11.0	-9493.3
15. C ₂ H ₅ + C ₂ H ₂ ⇒ C ₂ H ₃ + C ₂ H ₄	1.37E+32	-5.9	17783.4
16. CFBCCC ⇒ C ₂ H ₃ +C ₂ H ₄	5.31E+47	-10.8	41438.1
17. C ₂ H ₃ + C ₂ H ₄ ⇒ CFBCCC	1.05E+39	-8.8	15189.2
18. CFBCCC ⇒ C ₂ H ₅ + C ₂ H ₂	1.33E+35	-7.7	33711.0
19. C ₂ H ₅ + C ₂ H ₂ ⇒ CFBCCC	8.59E+25	-5.5	7425.2
20. CWCC + H ⇒ C ₂ H ₂ + CH ₃	3.94E+22	-2.9	10460.8
21. CWCC + H ⇒ CBCCF	1.43E+42	-8.9	16415.7
Declared duplicate reaction...			
22. CBCCF ⇒ C ₂ H ₂ + CH ₃	5.30E+45	-9.6	72167.7
23. C ₂ H ₂ + CH ₃ ⇒ CBCCF	2.64E+35	-7.2	20960.2
24. CWCC + H ⇒ CBCCF	3.15E+42	-9.1	16466.8
Declared duplicate reaction...			
25. CWCCF + H ⇒ CH ₂ + C ₂ H ₂	2.19E+15	-.6	13465.8
26. CH ₂ + C ₂ H ₂ ⇒ CWCCF + H	1.38E+10	.5	-123.8
27. CWCCF + H ⇒ C ₂ H + CH ₃	1.10E+16	-.7	33718.7
28. C ₂ H + CH ₃ ⇒ CWCCF + H	7.49E+08	.8	-3267.2
29. CWCC ⇒ CWCCF + H	2.04E+49	-10.2	103640.2
30. CWCCF + H ⇒ CWCC	2.85E+44	-9.2	11916.9
Declared duplicate reaction...			
31. CH ₂ + C ₂ H ₂ ⇒ CWCC	3.49E+39	-9.0	7388.7
32. CWCCF + H ⇒ CWCC	2.08E+39	-7.9	8358.0
Declared duplicate reaction...			
33. C ₂ H + CH ₃ ⇒ CWCC	1.42E+32	-6.4	-28628.0
34. C ₂ H ₃ + CH ₃ ⇒ CBCCF + H	4.25E+24	-3.1	11635.5
35. CBCCF + H ⇒ C ₂ H ₃ + CH ₃	8.40E+32	-4.8	26583.9
36. CBCC ⇒ CBCCF + H	1.37E+30	-4.5	94589.3
37. CBCCF + H ⇒ CBCC	2.13E+27	-4.0	4706.5
38. CWCCF + C ₂ H ₂ ⇒ CWCCCBCF	3.54E+28-6.0	9131.8	
39. CWCCCBCF ⇒ CWCCF + C ₂ H ₂	2.54E+37	-8.2	23655.7
40. CWCCF + C ₂ H ₂ ⇒ CY13PD1F	1.04E+49	-11.9	19017.8
41. CY13PD1F ⇒ CWCCF + C ₂ H ₂	3.66E+63	-15.0	71048.5
42. CWCCCBCF ⇒ CY13PD1F	1.49E+68	-18.4	28437.7
43. CBCCF + C ₂ H ₂ ⇒ CBCCCBCF	4.88E+12	-1.5	2644.8
44. CBCCCBCF ⇒ CBCCF + C ₂ H ₂	2.65E+21	-3.7	15179.5
45. CBCCF+C ₂ H ₂ ⇒ CWCCCBC + H	1.60E+04	2.1	25608.9
46. CWCCCBC + H ⇒ CBCCF + C ₂ H ₂	8.28E+09	.9	4266.2
47. CBCCCBCF ⇒ CWCCCBC + H	7.97E+13	-1.6	10753.9
48. CWCCCBC + H ⇒ CBCCCBCF	7.61E+10	-.6	-23123.6
49. CBCC + H ⇒ CBCCF + H ₂	4.42E+08	1.5	3938.0
50. CWCC + H ⇒ CWCCF + H ₂	4.42E+08	1.5	4253.0

Appendix A (continued)

CH ₄ -N ₂ Reduced mechanism		$(k = A T^{**} b \exp(-E/RT))$		
		A	b	E
51. CWCCF + H ₂ ⇒ CWCC + H		1.46E+04	2.5	16753.0
52. C ₂ H ₆ + H ⇒ C ₂ H ₅ + H ₂		1.44E+09	1.5	7412.0
53. C ₂ H ₅ + H ₂ ⇒ C ₂ H ₆ + H		3.18E+03	2.6	7714.8
54. CH ₄ + H ⇒ CH ₃ + H ₂		9.60E+08	1.5	9830.0
55. CH ₃ + H ₂ ⇒ CH ₄ + H		3.17E+04	2.3	6719.6
56. C ₂ H ₄ + H ⇒ C ₂ H ₃ + H ₂		9.60E+08	1.5	11452.0
57. C ₂ H ₃ + H ₂ ⇒ C ₂ H ₄ + H		8.38E+03	2.4	2486.6
58. H ₂ + C ₂ H ⇒ H + C ₂ H ₂		2.80E+10	.9	1900.0
59. H + C ₂ H ₂ ⇒ H ₂ + C ₂ H		6.78E+15	-.2	32171.7
60. H + CH ₃ (+M) ⇒ CH ₄ (+M)		3.48E+15	-.5	536.0
H ₂	Enhanced by	2.00E+00		
CH ₄	Enhanced by	3.00E+00		
C ₂ H ₆	Enhanced by	3.00E+00		
Low pressure limit		.26200E+34		
TROE centering		.78300E+00		.69640E+04
61. CH ₄ (+M) ⇒ H + CH ₃ (+M)		2.49E+20	-1.3	107869.7
H ₂	Enhanced by	2.00E+00		
CH ₄	Enhanced by	3.00E+00		
C ₂ H ₆	Enhanced by	3.00E+00		
Low pressure limit		.18770E+39		
TROE centering		.78300E+00		.69640E+04
62. H + C ₂ H ₃ (+M) ⇒ C ₂ H ₄ (+M)		6.08E+12	.3	280.0
H ₂	Enhanced by	2.00E+00		
CH ₄	Enhanced by	2.00E+00		
C ₂ H ₆	Enhanced by	3.00E+00		
Low pressure limit		.14000E+31		
TROE centering		.78200E+00		.60950E+04
63. C ₂ H ₄ (+M) ⇒ H + C ₂ H ₃ (+M)		1.65E+18	-.6	113468.7
H ₂	Enhanced by	2.00E+00		
CH ₄	Enhanced by	2.00E+00		
C ₂ H ₆	Enhanced by	3.00E+00		
Low pressure limit		.37980E+36		
TROE centering		.78200E+00		.60950E+04
64. CH + H ₂ (+M) ⇒ CH ₃ (+M)		1.97E+12	.4	-370.0
H ₂	Enhanced by	2.00E+00		
CH ₄	Enhanced by	2.00E+00		
C ₂ H ₆	Enhanced by	3.00E+00		
Low pressure limit		.48200E+26		
TROE centering		.57800E+00		.93650E+04
65. H + C ₂ H ₂ (+M) ⇒ C ₂ H ₃ (+M)		5.60E+12	.0	2400.0
H ₂	Enhanced by	2.00E+00		
CH ₄	Enhanced by	2.00E+00		
C ₂ H ₆	Enhanced by	3.00E+00		
Low pressure limit		.38000E+41		
TROE centering		.75070E+00		.41670E+04
66. C ₂ H ₃ (+M) ⇒ H + C ₂ H ₂ (+M)		5.69E+14	-.6	38659.1
H ₂	Enhanced by	2.00E+00		
CH ₄	Enhanced by	2.00E+00		
C ₂ H ₆	Enhanced by	3.00E+00		
Low pressure limit		.38600E+43		
TROE centering		.75070E+00		.41670E+04
67. H + C ₂ H ₄ (+M) ⇒ C ₂ H ₅ (+M)		5.40E+11	.5	1820.0
H ₂	Enhanced by	2.00E+00		
CH ₄	Enhanced by	2.00E+00		
C ₂ H ₆	Enhanced by	3.00E+00		
Low pressure limit		.60000E+42		
TROE centering		.97530E+00		.43740E+04

(continued on next page)

Appendix A (continued)

CH ₄ -N ₂ Reduced mechanism			$(k = A T^{**} b \exp(-E/RT))$		
			A	b	E
68. C ₂ H ₅ (+M) ⇒ H + C ₂ H ₄ (+M)			1.80E+13	.0	38042.1
H ₂	Enhanced by	2.000E+00			
CH ₄	Enhanced by	2.000E+00			
C ₂ H ₆	Enhanced by	3.000E+00			
Low pressure limit	.19950E+44	-.81000E+01	.43192E+05		
TROE centering	.97530E+00	.21000E+03	.98400E+03		.43740E+04
69. 2H + N ₂ ⇒ H ₂ + N ₂			5.40E+18	-1.3	.0
70. N + H + M ⇒ NH + M			1.02E+14	.1	-4735.9
71. NH + H ⇒ N + H ₂			3.20E+13	.0	325.0
72. N + H ₂ ⇒ NH + H			2.93E+13	.2	24312.4
73. NH + N ⇒ N ₂ + H			9.00E+11	.5	.0
74. N ₂ + H ⇒ NH + N			5.51E+13	.4	146093.9
75. NH + H ₂ ⇒ NH ₂ + H			1.00E+14	.0	20070.0
76. NH ₂ + H ⇒ NH + H ₂			4.79E+15	-.4	8711.3
77. N ₂ H ₃ + H ⇒ 2NH ₂			5.00E+13	.0	2000.0
78. NH + H ₂ + M ⇒ NH ₃ + M			6.70E+08	1.2	-5608.9
79. NH ₃ + H ⇒ NH ₂ + H ₂			5.42E+05	2.4	9920.0
80. NH ₂ + H ₂ ⇒ NH ₃ + H			6.53E+01	3.2	3785.7
81. N ₂ H ₃ + H ₂ ⇒ NH ₃ + NH ₂			4.57E+14	-.3	19169.3
82. NNH ⇒ N ₂ + H			3.00E+08	.0	.0
Declared duplicate reaction...					
83. N ₂ + H ⇒ NNH			5.12E+06	.6	5536.4
Declared duplicate reaction...					
84. NNH + M ⇒ N ₂ + H + M			1.00E+13	.5	3060.0
Declared duplicate reaction...					
85. N ₂ + H + M ⇒ NNH + M			1.71E+11	1.1	8596.4
Declared duplicate reaction...					
86. NNH + H ⇒ N ₂ + H ₂			1.00E+14	.0	.0
87. N ₂ + H ₂ ⇒ NNH + H			4.04E+12	.7	109759.6
88. N ₂ H ₂ + M ⇒ NNH + H + M			5.00E+16	.0	50000.0
N ₂	Enhanced by	2.000E+00			
H ₂	Enhanced by	2.000E+00			
89. NNH + H + M ⇒ N ₂ H ₂ + M			1.23E+12	.8	-11637.1
N ₂	Enhanced by	2.000E+00			
H ₂	Enhanced by	2.000E+00			
90. 2NH + M ⇒ N ₂ H ₂ + M			5.60E+08	1.4	-22558.7
N ₂	Enhanced by	2.000E+00			
H ₂	Enhanced by	2.000E+00			
91. N ₂ H ₂ + H ⇒ NNH + H ₂			8.50E+04	2.6	-230.0
92. 2N ₂ H ₂ ⇒ N ₂ H ₃ + NNH			4.70E+13	.1	-1836.9
93. N ₂ H ₃ + M ⇒ NH ₂ + NH + M			5.00E+16	.0	60000.0
94. NH ₂ + NH + M ⇒ N ₂ H ₃ + M			1.16E+07	2.0	-36568.2
95. N ₂ H ₃ + M ⇒ N ₂ H ₂ + H + M			1.00E+16	.0	37000.0
96. N ₂ H ₂ + H + M ⇒ N ₂ H ₃ + M			1.16E+12	1.0	-30474.0
97. N ₂ H ₃ + H ⇒ NH + NH ₃			1.00E+11	.0	.0
98. C ₂ H + HCN ⇒ CN + C ₂ H ₂			3.20E+120	.0	1530.0
99. CN + C ₂ H ₂ ⇒ C ₂ H + HCN			8.38E+13	-.2	10604.0
100. HCN + M ⇒ H + CN + M			3.57E+26	-2.6	124900.0
101. H + CN + M ⇒ HCN + M			1.63E+22	-1.7	-521.0
102. C ₂ N ₂ + M ⇒ 2CN + M			3.20E+16	.0	94400.0
103. 2CN + M ⇒ C ₂ N ₂ + M			2.48E+06	2.1	-40829.5
104. CN + NH ₃ ⇒ HCN + NH ₂			9.20E+12	.0	-357.0
105. CH + N ₂ ⇒ HCN + N			5.10E+11	.0	13600.0
106. HCN + N ⇒ CH + N ₂			2.46E+14	-.5	11113.2
107. C + N ₂ ⇒ CN + N			5.20E+13	.0	44700.0
108. CN + N ⇒ C + N ₂			7.07E+13	-.1	-726.7
109. HCN + NH ⇒ CH ₂ + N ₂			1.40E+14	-.4	11459.8
110. H ₂ CN + N ⇒ N ₂ + CH ₂			6.00E+13	.0	400.0
111. H ₂ CN + H ⇒ HCN + H ₂			2.40E+08	1.5	-894.0

Appendix A (continued)

CH ₄ -N ₂ Reduced mechanism	$(k = A T^{**} b \exp(-E/RT))$		
	A	b	E
112. HCN + H ₂ ⇒ H ₂ CN + H	3.72E+06	2.1	77247.2
113. H ₂ CN + M ⇒ HCN + H + M	3.00E+14	.0	22000.0
114. HCN + H + M ⇒ H ₂ CN + M	1.97E+12	.5	-4082.1
115. H ₂ CN + CH ₃ ⇒ HCN + CH ₄	8.10E+05	1.9	-1113.0
116. CH ₂ + N ⇒ HCN + H	5.00E+13	.0	.0
117. HCN + H ⇒ CH ₂ + N	8.95E+16	-6	121703.7
118. CH + N ⇒ CN + H	1.67E+14	-1	.0
119. CN + H ⇒ CH + N	5.83E+14	.0	98422.0
120. CH + N ⇒ C + NH	4.50E+11	.7	2400.0
121. C + NH ⇒ CH + N	1.88E+10	1.0	154.8
122. CH ₃ + N ⇒ H ₂ CN + H	7.10E+13	.0	.0
123. H ₂ CN + H ⇒ CH ₃ + N	3.13E+15	-4	36687.2
124. HCN + CH ₂ ⇒ C ₂ H ₃ + N	2.72E+10	.7	58893.1
125. CN + H ₂ ⇒ HCN + H	2.00E+04	2.9	1600.0
126. HCN + H ⇒ CN + H ₂	1.85E+08	1.9	22797.7
127. CN + HCN ⇒ C ₂ N ₂ + H	1.51E+07	1.7	1530.0
128. C ₂ N ₂ + H ⇒ CN + HCN	8.92E+12	.5	11338.5
129. CN + CH ₄ ⇒ HCN + CH ₃	9.00E+04	2.6	-300.0
130. HCN + CH ₃ ⇒ CN + CH ₄	2.75E+04	2.5	17787.3
131. C ₃ H ₃ + N ⇒ HCN + C ₂ H ₂	1.00E+13	.0	.0
132. HCN + C ₂ H ₂ ⇒ C ₃ H ₃ + N	4.88E+13	.8	109609.7
133. CH + N ₂ ⇒ NCN + H	5.10E+11	.0	13600.0
134. NCN + H ⇒ CH + N ₂	1.43E+16	-1.0	-16370.8
135. H + SCH ₂ ⇒ CH + H ₂	3.00E+13	.0	.0
136. CH + H ₂ ⇒ H + SCH ₂	3.28E+11	.4	11177.3
137. SCH ₂ + N ₂ ⇒ CH ₂ + N ₂	1.50E+13	.0	600.0
138. CH ₂ + N ₂ ⇒ SCH ₂ + N ₂	2.96E+12	.1	9693.4
139. SCH ₂ + H ₂ ⇒ CH ₃ + H	7.00E+13	.0	.0
140. CH ₃ + H ⇒ SCH ₂ + H ₂	3.61E+16	-7	15968.7
141. SCH ₂ + CH ₃ ⇒ H + C ₂ H ₄	1.20E+13	.0	-570.0
142. 2CH ₃ ⇒ SCH ₂ + CH ₄	2.73E+11	.2	12288.3
143. SCH ₂ + C ₂ H ₆ ⇒ CH ₃ + C ₂ H ₅	4.00E+13	.0	-550.0
144. SCH ₂ + N ₂ ⇒ NH + HCN	1.00E+11	.0	65000.0
145. NH + HCN ⇒ SCH ₂ + N ₂	5.76E+11	-4	49703.2
146. 2NH ⇒ N ₂ + 2H	5.13E+13	.0	.0

A units mol⁻¹ cm³ s⁻¹, E units cal/mol

Denotations: B: double bond; W: triple bond; F: free radical; SCH₂: singlet CH₂.

Note: Most of the reactions and their rate parameters were adopted from the butane pyrolysis mechanism. The reverse rate coefficients were calculated with MECHMOD.

References

- Bird, M.K., Dutta-Roy, R., Asmar, S.W., Rebold, T.A., 1997. Detection of Titan's ionosphere from Voyager 1 radio occultation observations. *Icarus* 130, 426–436.
- Borucki, W.J., McKay, C.P., Whitten, R.C., 1984. Possible production by lightning of aerosols and trace gases in Titan's atmosphere. *Icarus* 60, 260–273.
- Borucki, W., Giver, L.P., McKay, C.P., Scattergood, T., Parris, J.E., 1988. Lightning production of hydrocarbons and HCN on Titan: Laboratory measurements. *Icarus* 76, 125–134.
- Christian, H.J., 1999. Optical detection of lightning from space. In: Proceedings of the 11th International Conference on Atmospheric Electricity, Guntersville, Alabama, June 7–11, 1999, pp. 715–718.
- Coll, P., Coscia, D., Smith, N., Gazeau, M.-C., Ramírez, S.I., Cernogora, G., Israel, G., Raulin, F., 1999. Experimental laboratory simulations of Titan's atmosphere: Aerosol and gas phase. *Planet. Space Sci.* 47, 1331–1340.
- CRC Handbook of Chemistry and Physics, 1994–1995. Heat Capacity and Heat Conductivity Tables, 75th ed. CRC Press.
- Crespin, A., Lebonnois, S., Vinatier, S., Bezaud, B., Coustenis, A., Teanby, N.A., Achterberg, R.K., Rannou, P., Hourdin, F., 2008. Diagnostics of Titan's stratospheric dynamics using Cassini/CIRS data and the 2-dimensional IPSL circulation model. *Icarus* 197, 556–571.
- EQUIL, 2009. <<http://www.ca.sandia.gov/HiTempThermo/sample.html>>.
- Finke, U., 2007. Luftelektrizität, Institute für Meteorologie und Klimatologie, Universität Hannover, institutional seminar handouts.
- Fischer, G., Gurnett, D.A., Kurth, W.S., Farrell, W.M., Kaiser, M.L., Zarka, P., 2007. Nondetection of Titan lightning radio emissions with Cassini/RPWS after 35 close Titan flybys. *Geophys. Res. Lett.* 34, L22104.
- FluxViewer, 2007. <<http://garfield.chem.elte.hu/Combustion/fluxviewer.htm>>.
- Friend, D.G., Ely, J.F., Ingham, H., 1987. Viscosity and thermal conductivity of nitrogen for a wide range of fluid states. *J. Phys. Chem. Ref. Data* 16, 993–1023.
- Fujii, T., Arai, N., 1999. Analysis of N-containing hydrocarbon species produced by a CH₄/N₂ microwave discharge: Simulation of Titan's atmosphere. *Astrophys. J.* 519, 858–863.
- Fulchignoni, M., and 42 colleagues, 2005. In situ measurements of the physical characteristics of Titan's environment. *Nature* 438, 785–791.
- Gupta, G.K., Hecht, E.S., Zhu, H., Dean, A.M., Kee, R.J., 2006. Gas-phase reactions of methane and natural-gas with air and steam in non-catalytic regions of a solid-oxide fuel cell. *J. Power Sources* 156, 434–447.
- Izsák, F., Lagzi, I., 2005. A new universal law for the Liesegang pattern formation. *J. Chem. Phys.* 122, 184707.
- KINALC, 2005. <<http://garfield.chem.elte.hu/Combustion/software/kinalc.f>>.
- de Kok, R., Irwin, P.G.J., Teanby, N.A., 2008. Condensation in Titan's stratosphere during polar winter. *Icarus* 197, 572–578.
- Kovács, T., Deam, R.T., 2006. Methane reformation using plasma: An initial study. *J. Phys. D: Appl. Phys.* 39, 2391–2400.
- Kovács, T., Turányi, T., Föglein, K., Szépvölgyi, J., 2005. Kinetic modelling of the decomposition of carbon tetrachloride in thermal plasma. *Plasma Chem. Plasma Process.* 25, 109–119.

- Kovács, T., Turányi, T., Föglein, K., Szépvölgyi, J., 2006. Modelling of carbon tetrachloride decomposition in oxidative RF thermal plasma. *Plasma Chem. Plasma Process.* 26, 293–318.
- Landau, L.D., Lifshitz, E.M., 1987. *Course of Theoretical Physics. Fluid Mechanics*, vol. 6, second ed. Reed Educational and Professional Publishing Ltd.
- Lorenz, R.D., 1995. Raindrops on Titan. *Adv. Space Res.* 15, 317–320.
- Lutz, A.E., Kee, R.J., Miller, J.A., 1988. SENKIN. Sandia National Laboratories Report 87-8248.
- McEwan, M.J., Scott, G.B.I., Anicich, V.C., 1998. Ion-molecule reactions relevant to Titan's ionosphere. *Int. J. Mass Spectrom. Ion Process.* 172, 209–219.
- McGraw Hill, 1997. *Encyclopedia of Science and Technology*, vol. 74. McGraw Hill, p. 509.
- McKay, C.P., Martin, S.C., Griffith, C.A., Keller, R.M., 1997. Temperature lapse rate and methane in Titan's troposphere. *Icarus* 129, 498–505.
- MECHMOD, 2003. <<http://garfield.chem.elte.hu/Combustion/software/mechmod142.f>>.
- Niemann, H.B., and 17 colleagues, 2005. The abundances of constituents of Titan's atmosphere from the GCMS instrument on the Huygens probe. *Nature* 438, 779–784.
- Pereira, J., Massereau-Guilbaud, V., Geraud-Grenier, I., Plain, A., 2008. Nitrogen effect on the dust present and behaviour in a radio frequency CH₄/N₂ discharge. *J. Appl. Phys.* 103, 033301.
- Plankensteiner, K., Reiner, H., Rode, B.M., Mikoviny, T., Wisthaler, A., Hansel, A., Maerk, T.D., Fischer, G., Lammer, H., Rucker, H.O., 2007. Discharge experiments simulating chemical evolution on the surface of Titan. *Icarus* 187, 616–619.
- Revel, J., Boettner, J.C., Cathonnet, M., Bachman, J.S., 1994. Derivation of a global chemical kinetic mechanism for methane ignition and combustion. *J. Chim. Phys. Phys. Chim. Biol.* 91, 365–382.
- Romanzin, C., Benilan, Y., Jolly, A., Gazeau, M.-C., 2008. Photolytic behaviour of methane at Lyman-alpha and 248 Nm: Studies in the frame of a simulation program of Titan's atmosphere (setup). *Adv. Space Res.* 42, 2036–2044.
- SEM, 2009. <www.chem.elte.hu/Combustion/SEM.html>.
- Sheng, C.Y., Dean, A.M., 2004. The importance of gas phase kinetics within the anode channel of a solid-oxide fuel cell. *J. Phys. Chem. A* 108, 3772–3783.
- Stephen, K., Krauss, R., Laesecke, A., 1989. Thermophysical properties of methane. *J. Phys. Chem. Ref. Data* 18, 583–638.
- Tokano, T., Molina-Cuberos, G.J., Lammer, H., Stumtner, W., 2001. Modelling of thunderclouds and lightning generation on Titan. *Planet. Space Sci.* 49, 539–560.
- Tokano, T., McKay, C.P., Neubauer, F.M., Atreya, S.K., Ferri, F., Fulchignoni, M., Niemann, H.B., 2006. Methane drizzle on Titan. *Nature* 442, 432–435.
- Zsély, I.Gy., Zádor, J., Turányi, T., 2008. Uncertainty analysis of NO production during methane combustion. *Int. J. Chem. Kinet.* 40, 754–768.